

Supporting Information

Supported Ultrafine NiPt-MoO_x Nanocomposite as Highly Efficient Catalysts for Complete Dehydrogenation from Hydrazine Borane

Xia Kang, Jia-Xin Yao, Yan-Xin Duan, Ze-Yu Chen, Jun-Min Yan, * Qing Jiang

Key Laboratory of Automobile Materials, Ministry of Education, School of Materials Science and Engineering, Jilin University, Changchun, 130022, China

Chemicals

Graphite flake (C, 325 mesh, 99.8%) was obtained from Alfa Aesar. Sulfuric acid (H_2SO_4 , 98%) hydrogenperoxide (H_2O_2 , 30%) were obtained from Beijing Chemical Works. Phosphoric acid (H_3PO_4 , 85%), potassium chloroplatinate (K_2PtCl_4 , Pt > 45%), nickel chloride hexahydrate ($\text{NiCl}_2 \cdot 6\text{H}_2\text{O}$, 98%), sodium borohydride (NaBH_4 , 96%), n-pentane (C_5H_{12} , $\geq 99\%$), 1,4-dioxane ($\text{C}_4\text{H}_8\text{O}_2$, $\geq 99.5\%$) and hydrogen chloride (HCl, 37%) were bought from Sinopharm Chemical Reagent Co., Ltd. (3-Aminopropyl) triethoxysilane (APTS, $\text{C}_9\text{H}_{23}\text{NO}_3\text{Si}$, 99%), sodium hydroxide (NaOH, 96%) and potassium permanganate (KMnO_4 , >99.99%) were provided by Aladdin Chemistry Co., Ltd. Hydrazine hemisulfate salt ($\text{N}_2\text{H}_4 \cdot 1/2\text{H}_2\text{SO}_4$, 98%) were obtained from Sigma-Aldrich, The deionized water with a specific resistance of $18.2 \text{ M}\Omega \cdot \text{cm}$ was obtained by reverse osmosis followed by ion-exchange and filtration. All chemicals were used as received without further purification.

Synthesis procedure

GO was synthesized according to literature ¹ and the synthesis of NH_2 -N-rGO was based on our previous work. ² For preparation of $\text{Ni}_{0.9}\text{Pt}_{0.1}\text{-MoO}_x/\text{NH}_2\text{-N-rGO}$ (**Scheme 1**), APTS (0.2 mL) was added into the GO aqueous solution (3 mg/mL, 5 mL) accompanying with ultrasound treatment at 298 K for 10 minutes. And then, $\text{NiCl}_2 \cdot 6\text{H}_2\text{O}$ (0.1 M, 0.9 mL), K_2PtCl_4 (0.05 M, 0.2 mL) and Na_2MoO_4 (0.1 M, 1 mL) were put into the mixture with magnetic stirring. Finally, NaBH_4 (32.0 mg) was quickly added to the above mixture for reduction under stirring to obtain $\text{Ni}_{0.9}\text{Pt}_{0.1}\text{-MoO}_x/\text{NH}_2\text{-N-rGO}$. The system of $\text{Ni}_{0.9}\text{Pt}_{0.1}\text{-(MoO}_x)_y/\text{NH}_2\text{-N-rGO}$ with different molar ratios of $n_{\text{Mo}}/n_{\text{(Ni+Pt)}}$ were also obtained as the above way by altering the addition content of Na_2MoO_4 . ($n_{\text{Ni+Pt}} = 0.1 \text{ mmol}$, $n_{\text{Mo}} = 0, 0.05, 0.1, 0.15, 0.2$ and 0.25 mmol)

Compared to common nitrogen sources such as ethylenediamine,³ melamine⁴ and ammonia,⁵ APTS can introduce NH_2 and N together at room temperature in a short time, and the bifunctional group can lead to the better hydrophilicity than a single one.⁶

Syntheses of HB

Hydrazine borane (HB, $\text{N}_2\text{H}_4\text{BH}_3$) was prepared according to the reported literature. ⁷ Firstly, 32.81 g of $\text{N}_2\text{H}_4 \cdot 1/2\text{H}_2\text{SO}_4$ and 15.31 g of NaBH_4 were added into two-necked flask. Then, 120 mL of anhydrous dioxane was added to two-necked flask. The mixture was stirred under an atmosphere of Ar for 48 h at 298 K. Finally, white muddy product was centrifuged, and the supernatant was put in vacuum at 313 K. The obtained white solid was washed with n-pentane and dried under vacuum at 313 K, then we can get the target product.

Syntheses of GO

Graphene oxide (GO) was synthesized according to previous literature,¹ briefly, a certain amount of graphite (3.0 g) together with KMnO_4 (18.0 g) were put to the $\text{H}_2\text{SO}_4/\text{H}_3\text{PO}_4$ (360/40 mL) solution little by little. Then, the obtained hybrid was put into water bath at 323 K and mixed overnight (12 h). Subsequently, the hot mixture was cooled to 298 K. In order to add H_2O_2 (15~30 mL) and deionized water, ice was added to dilute it. Notably, the temperature must be controlled below 323 K. After that, the suspension was centrifuged (11000 r/min for 4 min),

then water and HCl (100 mL) were put into the trace solid material and mixed for 12 h. The obtained mixture was centrifuged (11000 r/min) 10 times with deionized water. Finally, GO aqueous solution was obtained by ultrasonication of the washed suspension for 40 min.

Catalytic reactions of hydrazine borane.

Typically, A flask consist of the mixture of catalysts and NaOH were used to start the reactions at 323 K under ambient atmosphere. The amount of HB participating in the reaction was fixed at 1 mmol (0.5 M, 2 mL). The concentration of NaOH was kept at 1.5 M. The reaction started when HB was poured into the reactor. The generated gas was measured by the burette. A HCl trap (0.1 M) was put between the flask and gas burette to remove the influence of any releasing NH_3 . Notably, when testing the influence of temperature, you only need to adjust the temperature of the corresponding water bath. For recycle tests, after the reaction of HB dehydrogenation was accomplished, another equivalent of HB (0.5 M, 2 mL) and the corresponding quantity of NaOH were subsequently put to the flask to start the reaction. The concentration of NaOH was always kept at 1.5 M. The released gas was measured by the gas burette. The rest of the operation is the same as that described on the front panel.

Characterizations

The X-ray diffraction (XRD) tests were measured on D/Max 2500pc diffractometer (Cu $\text{K}\alpha$, 50 kV, 200 mA, $\lambda = 1.54056 \text{ \AA}$), which was produced by Rigaku Electric Co., Ltd. ;Transmission electron microscopy (TEM) were using JEM-2100F microscopy (200 keV), which was produced by Nippon Technology Co., Ltd.; X-ray photoelectron spectroscopy (XPS) were measured on ESCALAB — 250Xi with the monochromatized Al $\text{K}\alpha$ as excitation source which was produced by Thermo Fisher; FTIR spectra were analyzed by 6800-50/NEXUS spectrometer, which was produced by Nicolli. Raman spectra were obtained through Renishaw, which was produced by Renishaw booth. UV-Vis absorption spectra were used to characterize the reduction of GO, and the equipment model was Agilent Cary 50 spectrophotometer, and the wavelength range was characterized was about 210-700 nm. Cary 50 was produced by Agilent Technologies Co., Ltd. MS measurement was carried out on OmniStar GSD320 mass spectrometer, which was produced by Pfeiffer Vacuum Technology Co., Ltd. and the carrying gas was Ar.

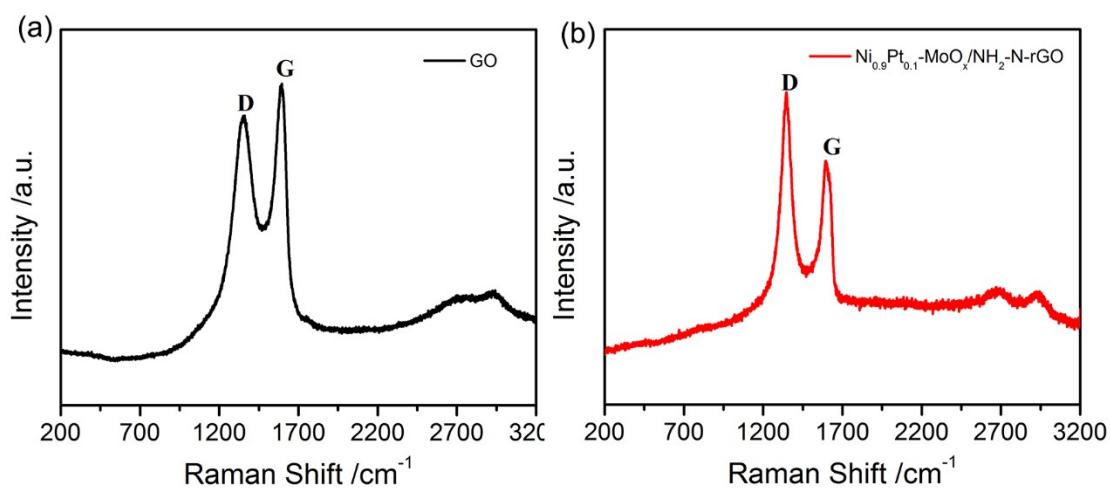


Fig. S1. Raman spectra of a) GO and b) Ni_{0.9}Pt_{0.1}-MoO_x/NH₂-N-rGO.

From Raman spectra of Ni_{0.9}Pt_{0.1}-MoO_x/NH₂-N-rGO and GO. The intensity ratio of D belt (1348 cm⁻¹) to G belt (1595 cm⁻¹) increases significantly, indicating the formation of rGO during the reduction reaction. ⁸

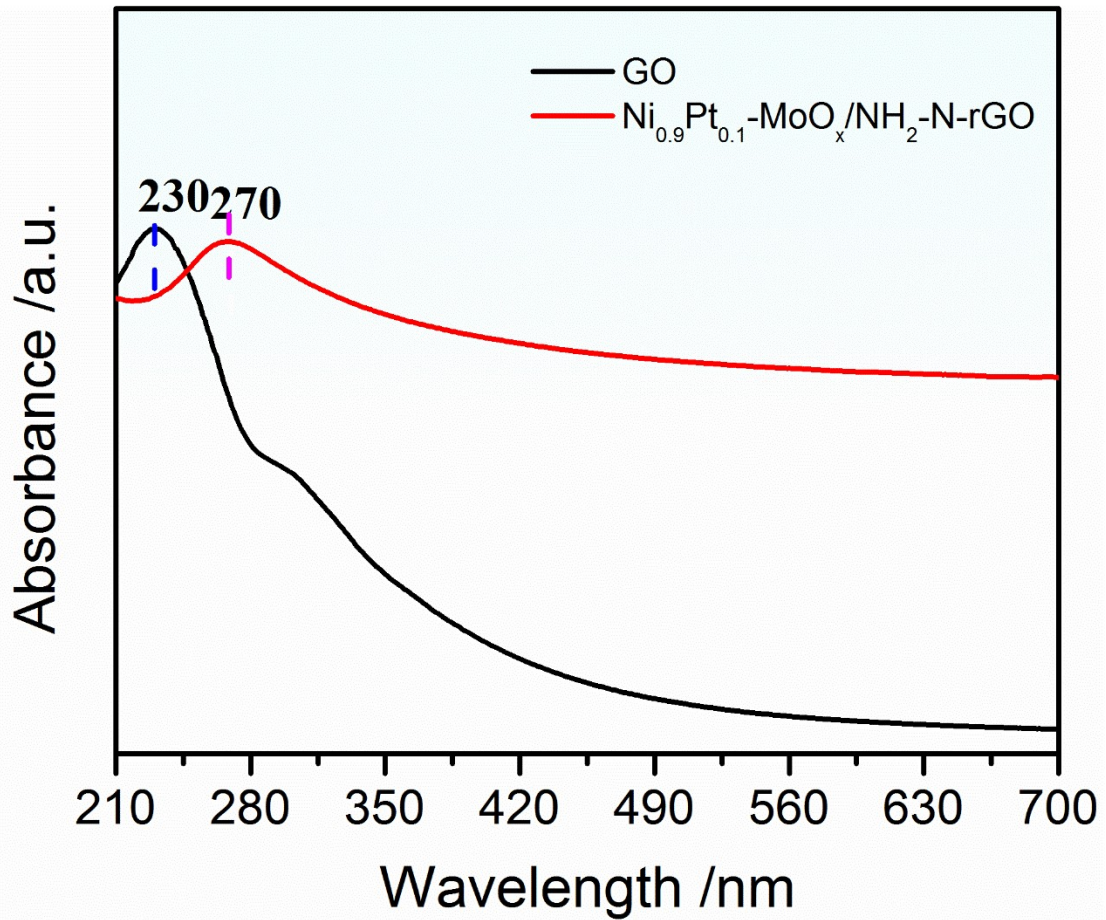


Fig. S2. UV-Vis absorption spectra of GO and $\text{Ni}_{0.9}\text{Pt}_{0.1}\text{-MoO}_x/\text{NH}_2\text{-N-rGO}$.

The peak of GO at 230 nm is red shifted to 270 nm after reduction, which confirms the effective reduction of GO to rGO during the synthesis of the $\text{Ni}_{0.9}\text{Pt}_{0.1}\text{-MoO}_x/\text{NH}_2\text{-N-rGO}$.⁸

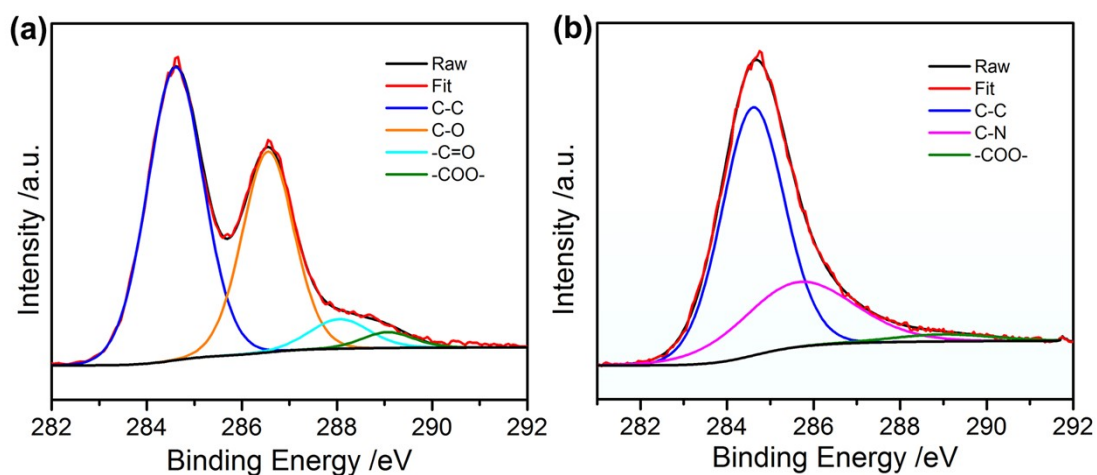


Fig. S3. High-resolution XPS spectra of C 1s in a) GO and b) Ni_{0.9}Pt_{0.1}-MoO_x/NH₂-N-rGO.

There are some oxygen-containing groups (C-O, 286.5 eV; -C=O, 288.0 eV; -COO-, 289.0 eV) in GO.⁹ In contrast to GO, most of the oxygen-containing groups (C-O, -C=O) in Ni_{0.9}Pt_{0.1}-MoO_x/NH₂-N-rGO (**Fig. S3b**) have been removed, and the -COO- group are decreased greatly. Indicating the successful reduction of GO to rGO², which also agrees well with the UV-vis and Raman results. Besides, owing to the production of C-N&C-OH, the peak centered at 285.4 eV in Ni_{0.9}Pt_{0.1}-MoO_x/NH₂-N-rGO is formed.¹⁰

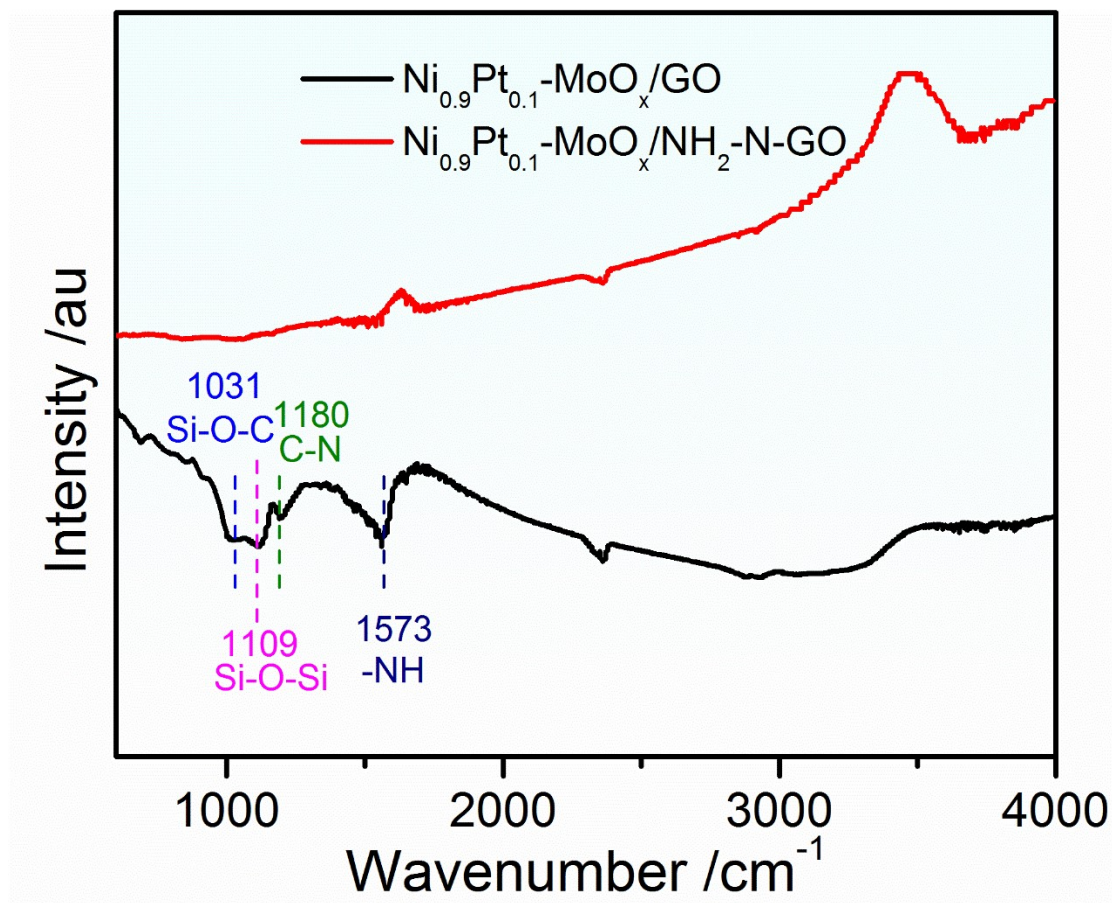


Fig. S4. FTIR spectra of Ni_{0.9}Pt_{0.1}-MoO_x/NH₂-N-rGO and Ni_{0.9}Pt_{0.1}-MoO_x/rGO.

Fourier transform infrared spectroscopy (FTIR) has been performed for Ni_{0.9}Pt_{0.1}-MoO_x/NH₂-N-rGO and Ni_{0.9}Pt_{0.1}-MoO_x/rGO. As displayed in Fig. S4, comparing Ni_{0.9}Pt_{0.1}-MoO_x/NH₂-N-rGO with Ni_{0.9}Pt_{0.1}-MoO_x/rGO, some peaks of Si-O-C (1031cm⁻¹), Si-O-Si (1109 cm⁻¹), C-N (1180 cm⁻¹) and -NH (1573 cm⁻¹) appeared, indicating the amine (-NH₂) group and N element have been successfully incorporated into the rGO of this sample.¹¹

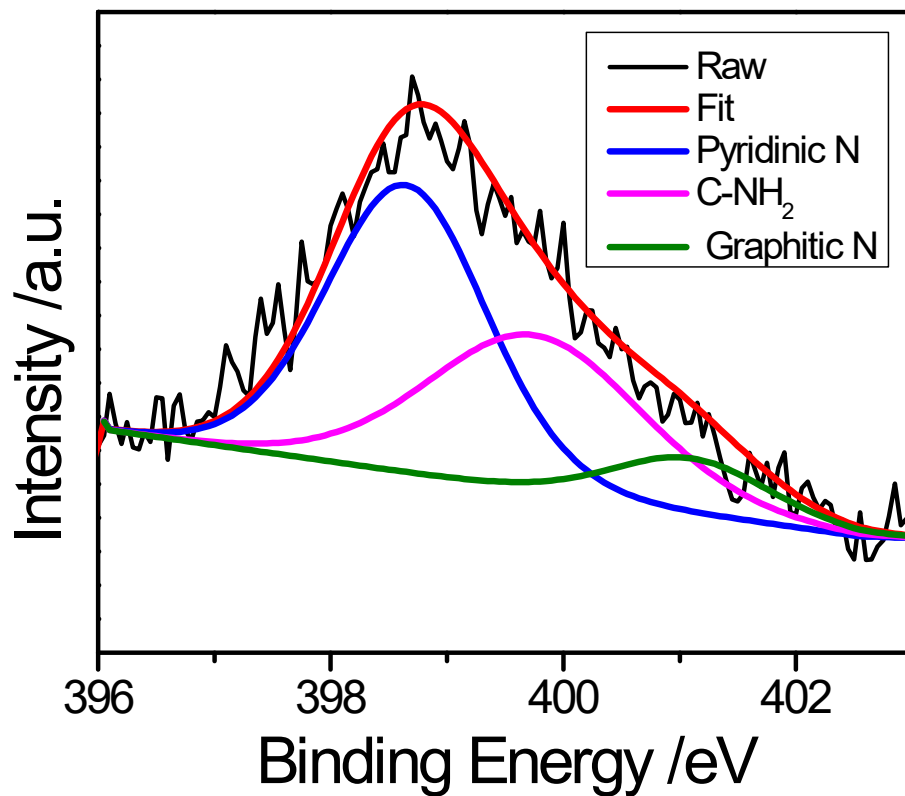


Fig. S5. High-resolution XPS spectrum of N1s in $\text{Ni}_{0.9}\text{Pt}_{0.1}\text{-MoO}_x/\text{NH}_2\text{-N-rGO}$.

As illustrated in Fig. S5, the peaks of N 1s for $\text{Ni}_{0.9}\text{Pt}_{0.1}\text{-MoO}_x/\text{NH}_2\text{-N-rGO}$ / $\text{NH}_2\text{-N-rGO}$ are observed at about ~ 400.0 eV, demonstrating the presence of pyridinic N (398.7 eV), C-NH₂ & pyrrolic N (399.7 eV) and graphitic N (401.1 eV),¹²⁻¹⁴ which also proves that the amine (-NH₂) group and N element have been successfully incorporated into the rGO of this sample.

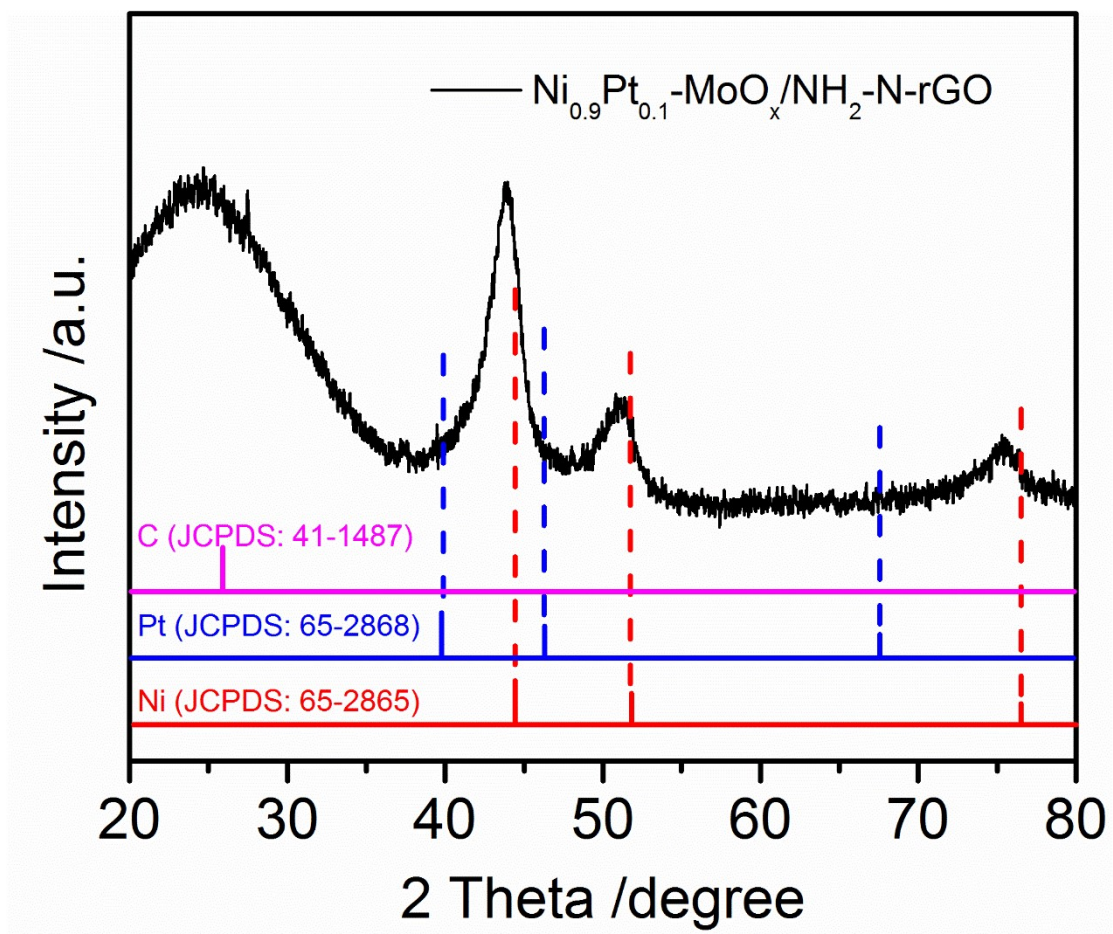


Fig. S6. XRD patterns of $\text{Ni}_{0.9}\text{Pt}_{0.1}\text{-MoO}_x/\text{NH}_2\text{-N-rGO}$ after heat treatment at 873 K for 3 h in Ar atmosphere

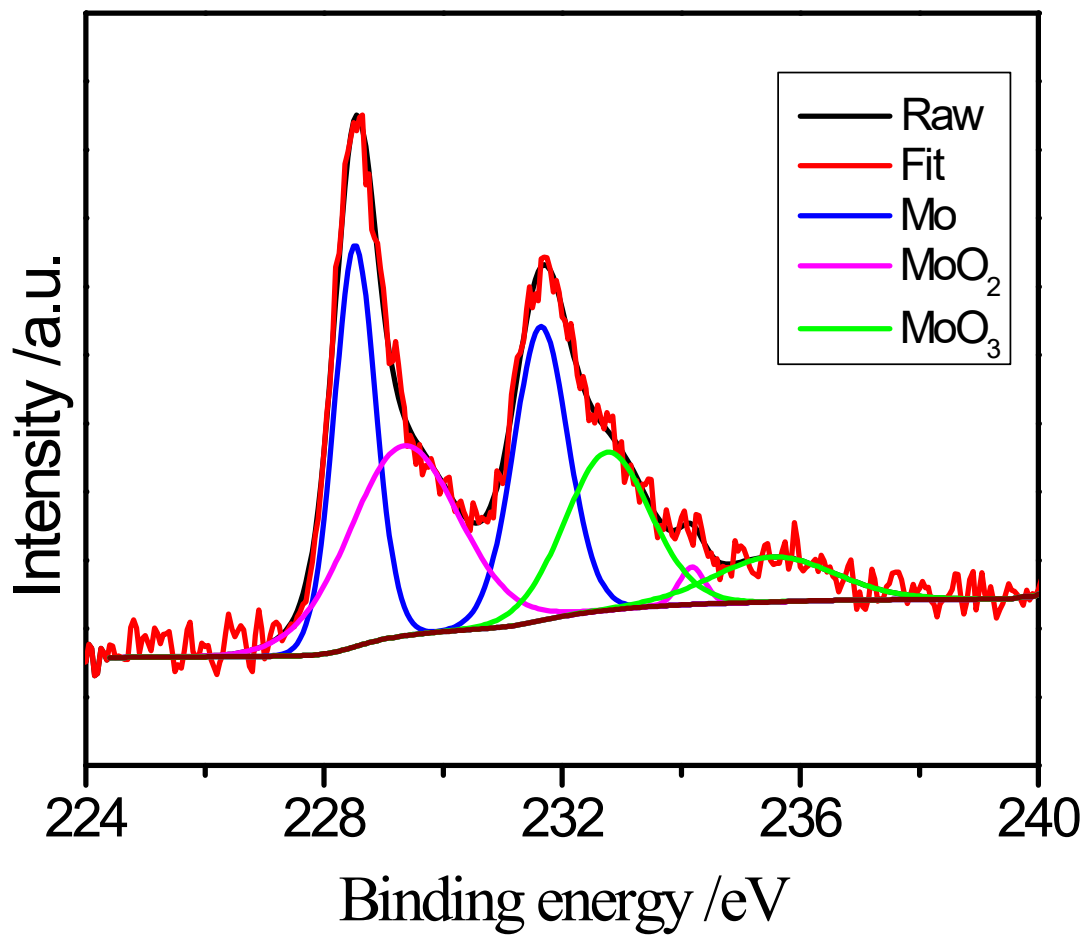


Fig. S7. XPS spectrum of Mo 3d for Ni_{0.9}Pt_{0.1}-MoO_x/NH₂-N-rGO composite.

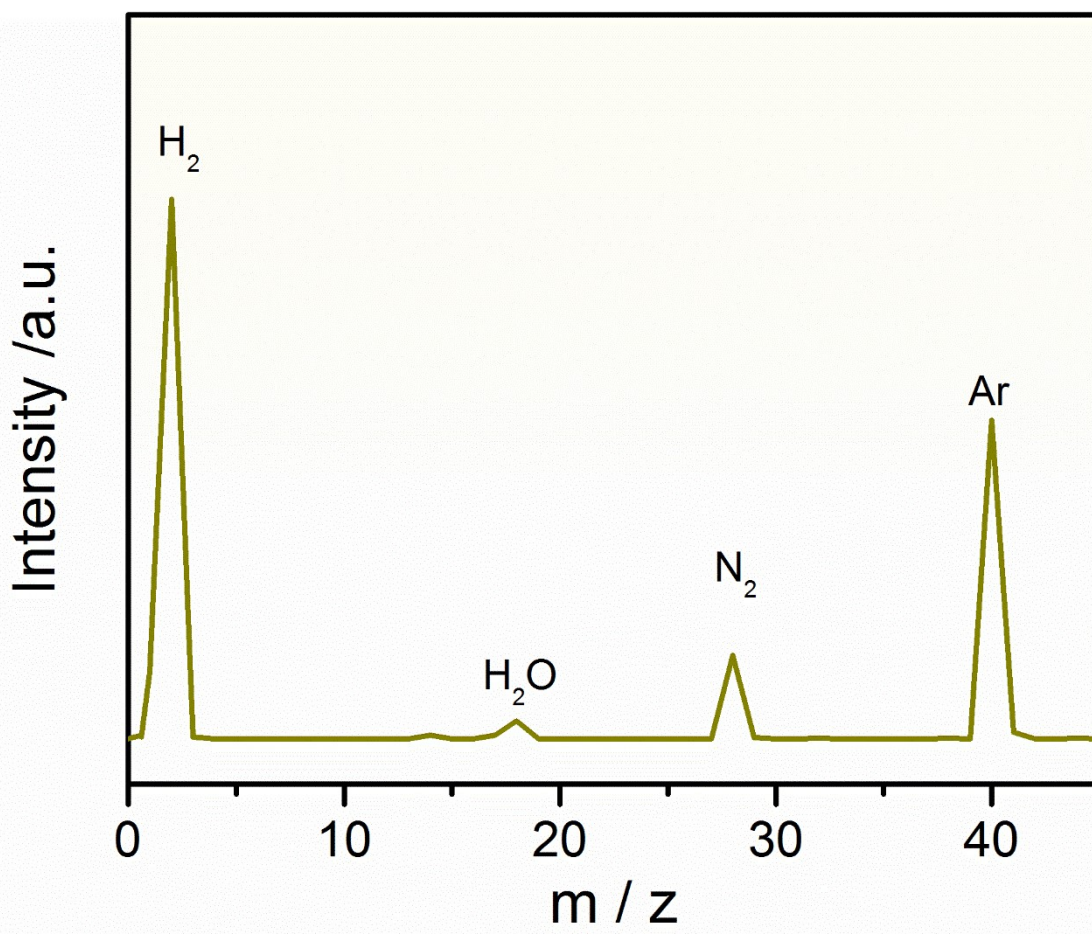


Fig. S8. Mass spectrum of released gases from the complete decomposition of HB catalyzed by Ni_{0.9}Pt_{0.1}-MoO_x/NH₂-N-rGO hybrid in Ar atmosphere at 323 K.

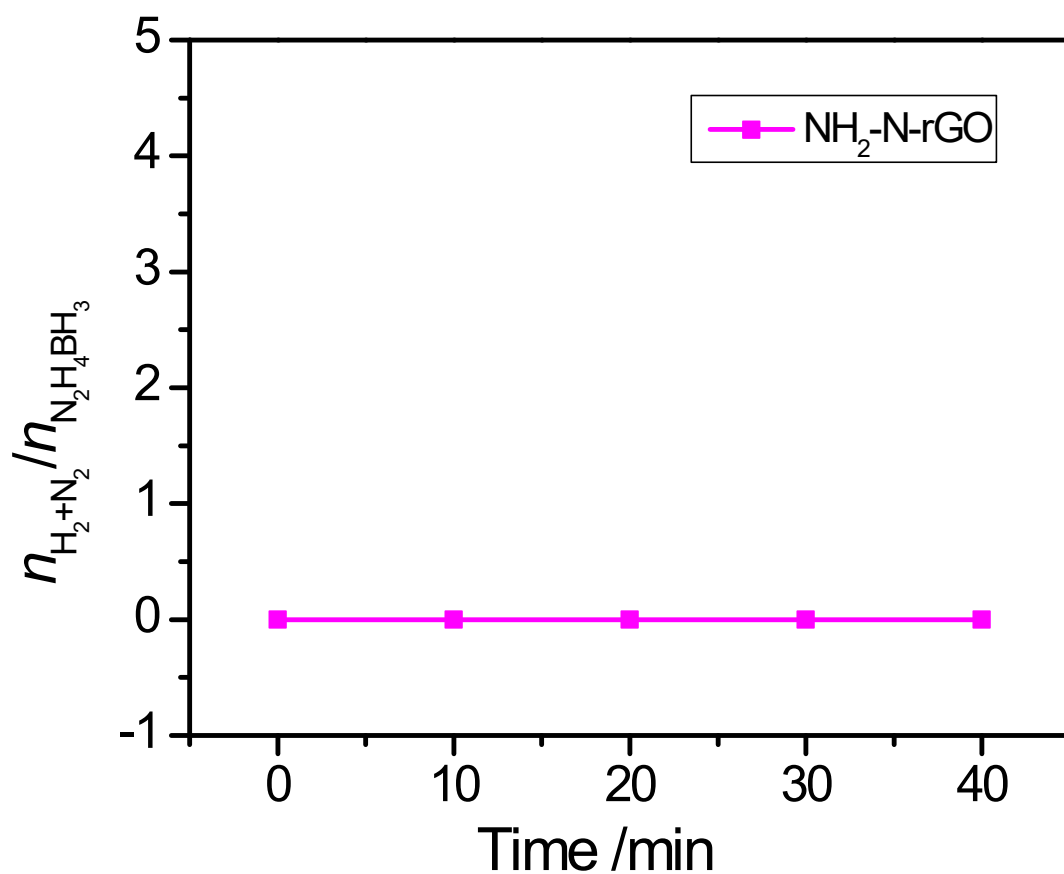


Fig. S9. Time-course plots for the decomposition of HB catalyzed by NH₂-N-rGO at 323 K.

It can be seen from the Fig. S9 that even after 40 minutes, NH₂-N-rGO as a catalyst does not produce hydrogen, indicating that NH₂-N-rGO is inactive for the dehydrogenation of HB.

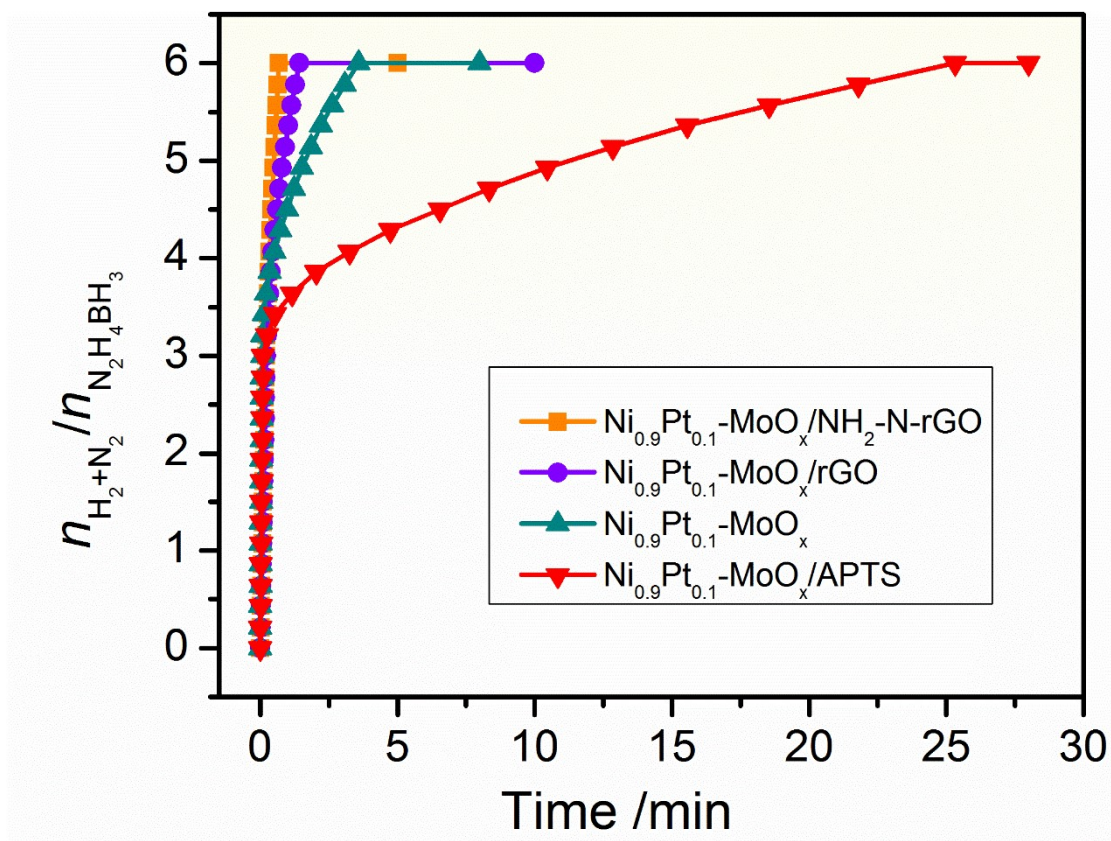


Fig. S10. Gas generation from the decomposition of HB (0.5 M, 2.0 mL) versus time in the presence of different catalysts

To better understand the influence of APTS and rGO on the catalytic activity of HB, Ni_{0.9}Pt_{0.1}-MoO_x/NH₂-N-rGO, Ni_{0.9}Pt_{0.1}-MoO_x/rGO, Ni_{0.9}Pt_{0.1}-MoO_x/APTS and Ni_{0.9}Pt_{0.1}-MoO_x are prepared using the same method. As shown in Fig. S10, without carrier, the free Ni_{0.9}Pt_{0.1}-MoO_x shows poor catalytic performance, 6.0 equiv. of H₂+N₂ can be obtained in 3.58 min, obtaining a TOF value of 838 h⁻¹. Ni_{0.9}Pt_{0.1}-MoO_x/APTS can release 6.0 equiv. of H₂+N₂ within 25.33 min, corresponding to the TOF value of only 118 h⁻¹. Moreover, for Ni_{0.9}Pt_{0.1}-MoO_x/rGO, the reaction can be completed in 1.43 min with a TOF value of 2098 h⁻¹, which is still inferior to the Ni_{0.9}Pt_{0.1}-MoO_x/NH₂-N-rGO (TOF value is 4412 h⁻¹).

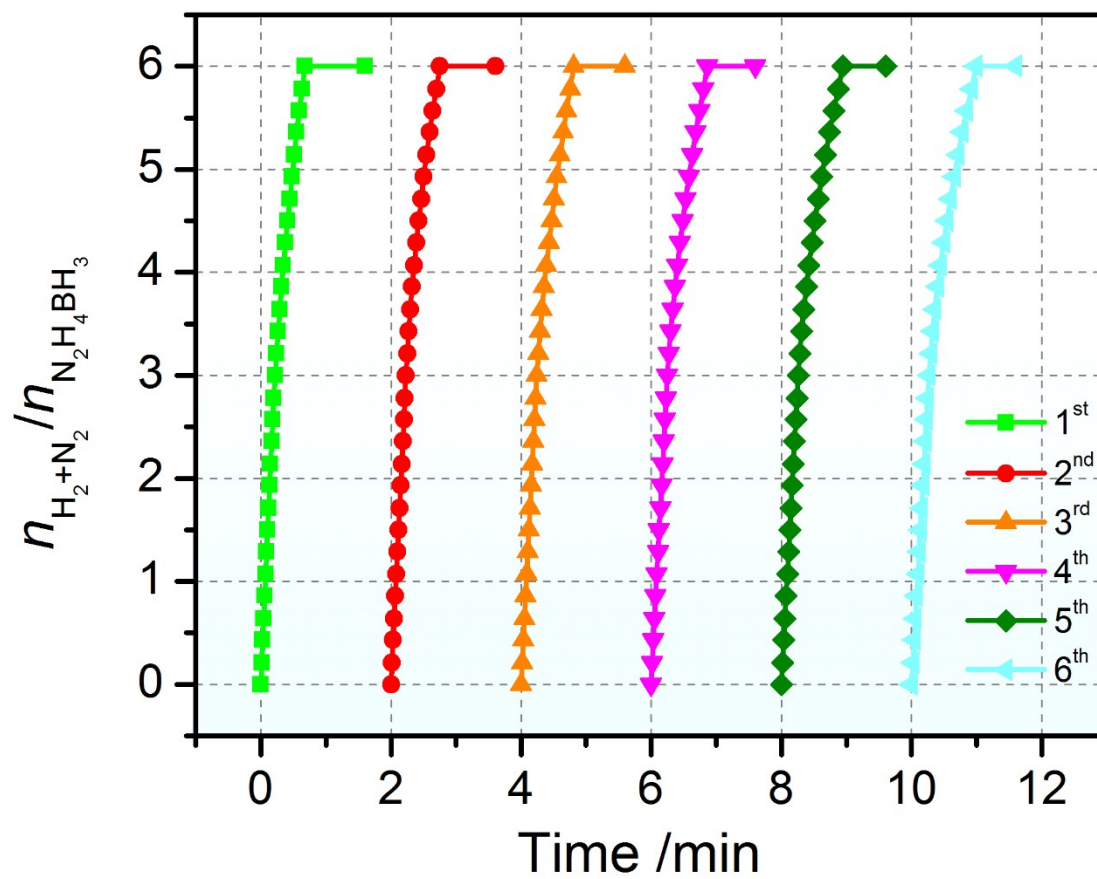


Fig. S11. Recycle test of the $\text{Ni}_{0.9}\text{Pt}_{0.1}\text{-MoO}_x/\text{NH}_2\text{-N-rGO}$ nanocatalyst toward the decomposition of HB at 323 K under ambient atmosphere. ($n_{\text{Ni+Pt}} = 0.1 \text{ mmol}$).

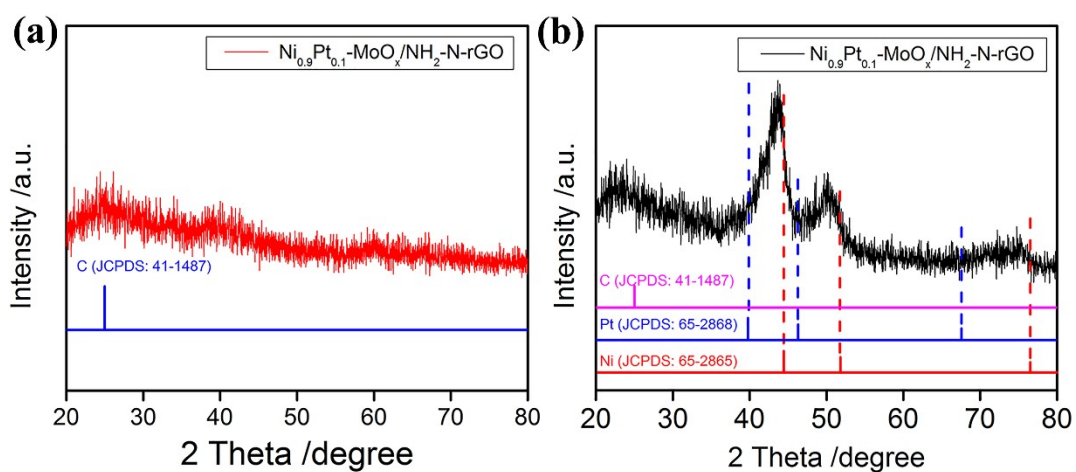


Fig. S12. XRD patterns for (a) Ni_{0.9}Pt_{0.1}-MoO_x/NH₂-N-rGO after the recycle test and (b) Ni_{0.9}Pt_{0.1}-MoO_x/NH₂-N-rGO after the recycle test and annealing at 873 K for 3h.

The XRD pattern of Ni_{0.9}Pt_{0.1}-MoO_x/NH₂-N-rGO after the reaction is the same as the one before the reaction, and there is no obvious diffraction peak for the metal (**Fig. S12a**). After annealing, the peak of the NiPt alloy appears (**Fig. S12b**), which is consistent with the structure before the reaction.

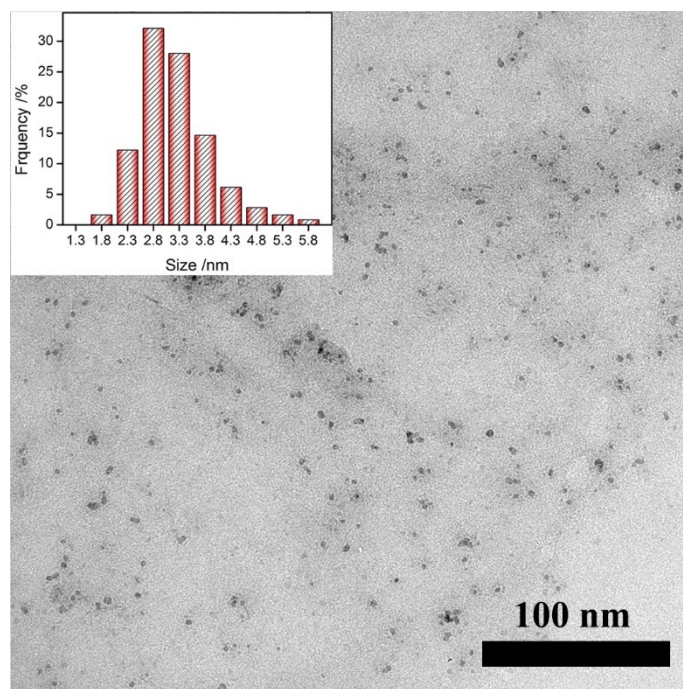


Fig S13. TEM image for $\text{Ni}_{0.9}\text{Pt}_{0.1}\text{-MoO}_x/\text{NH}_2\text{-N-rGO}$ after the recycle test, and the inset is the corresponding size distribution.

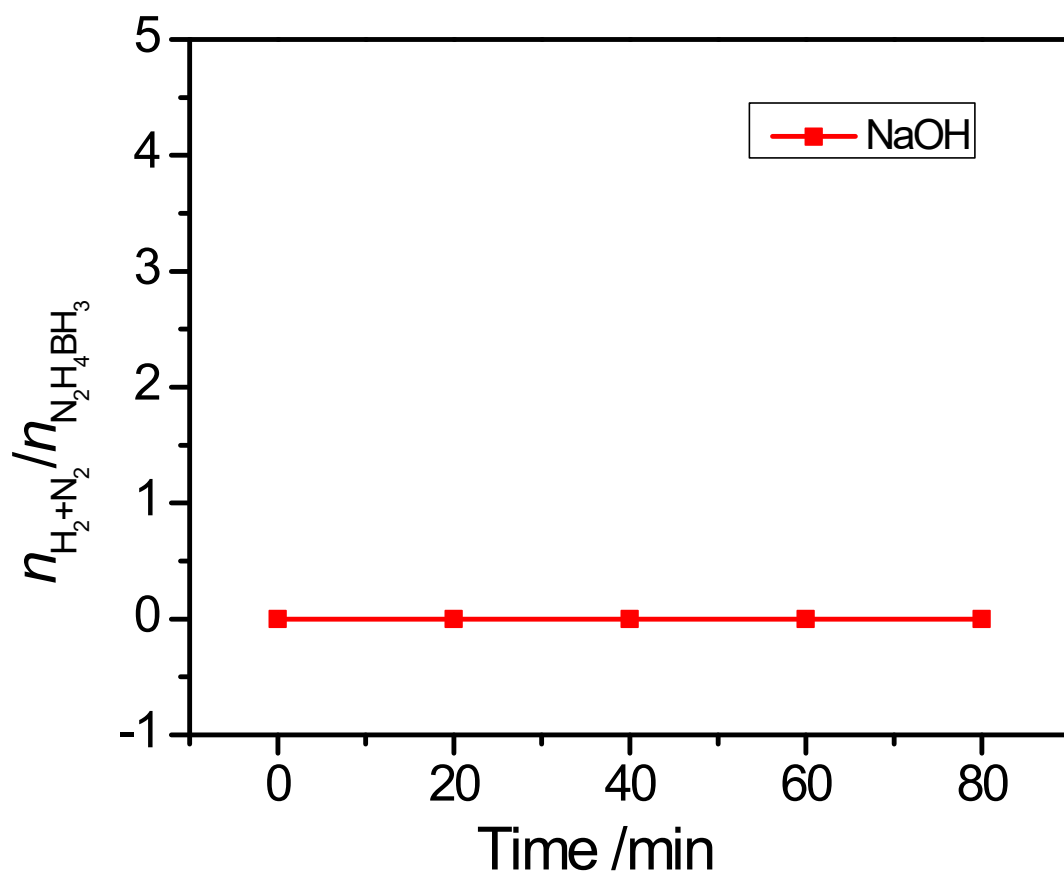


Fig. S14. Time-course plots for the decomposition of HB catalyzed by NaOH.

Calculation methods:

$$TOF = \frac{n_{H_2}}{n_{metal}t}$$

Where TOF is the total turnover frequency, n_{H_2} represent the mole amount of hydrogen (H₂) produced, n_{metal} represent the mole amount of active metal, and t is the total time to complete the reaction.¹⁵

The connection between temperature and speed, which can be called Arrhenius regulation. The Arrhenius' reaction speed could use the follow formula:^{16,17}

$$\ln TOF = \ln A - E_a / RT$$

Where A is the reaction constant.

Table S1. Performance toward different catalysts and the corresponding TOF values for HB dehydrogenation.

Catalyst	Temp. (K)	Reaction time (min)	$n(\text{H}_2+\text{N}_2)/n(\text{N}_2\text{H}_4\text{BH}_3)$	Conversion	TOF (h^{-1})	Ref.
$\text{Ni}_{0.9}\text{Pt}_{0.1}\text{-MoO}_x/\text{NH}_2\text{-N-rGO}$	323	0.68	6.0	100%	4412	This work
$\text{Ni}_{0.3}\text{Pt}_{0.7}\text{-Cr}_2\text{O}_3$	323	2.5	6.0	100%	3093	18
$\text{Ni}_{0.9}\text{Pt}_{0.1}\text{-Cr}_2\text{O}_3$	323	0.97	6.0	100%	1200	18
$\text{Ni}_{0.22}\text{@Ir}_{0.78}/\text{OMS-2}$	323	None	6.0	100%	2590	19
$\text{Rh}_{0.5}(\text{MoO}_x)_{0.5}$	323	1.5	6.0	100%	2000	20
$\text{Ni}_{0.75}\text{Ir}_{0.25}/\text{La}_2\text{O}_2\text{CO}_3$	323	2.4	6.0	100%	1250	21
$\text{Rh}_{0.8}\text{Ni}_{0.2}/\text{MIL-101}$	323	2.5	6.0	100%	1200	22
$\text{Ni}_{0.9}\text{Pt}_{0.1}/\text{MIL-101}$	323	1.95	6.0	100%	1515	23
$\text{Ni}_{0.9}\text{Pt}_{0.1}/\text{MIL-101}/\text{rGO}$	323	1.9	6.0	100%	1578	24
$\text{Rh}_{0.8}\text{Ni}_{0.2}\text{@CeO}_x/\text{rGO}$	323	4.5	6.0	100%	666.7	25
$\text{Ni-MoO}_x/\text{BN}$	323	5	6.0	100%	600	26
$\text{Ni}_{0.9}\text{Pt}_{0.1}/\text{graphene}$	323	12.5	6.0	100%	240	27
$\text{Cu}_{0.4}\text{Ni}_{0.6}\text{Mo}$	323	13.9	6.0	100%	108	28
$\text{Rh}_4\text{Ni NPs}/\text{CTAB}$	323	30	6.0	100%	90.9	29
$\text{Ni}_{0.36}\text{Fe}_{0.24}\text{Pd}_{0.4}/\text{MIL-101}$	323	25	6.0	100%	60	30
$\text{Ni}_{0.6}\text{Pd}_{0.4}\text{-MoO}_x$	323	7.33	5.92	98.7%	405	31
$\text{Ni}_{0.89}\text{Pt}_{0.11}\text{ NPs}/\text{CTAB}$	323	130	5.84	97.3%	18	32
$\text{Ni}(\text{Rh}_4\text{Ni-alloy})/\text{Al}_2\text{O}_3$	323	40	5.74	95.7%	71.7	33
$\text{Ni}_{0.9}\text{Pt}_{0.1}\text{-CeO}_2$	323	12.3	5.74	95.7%	234	34
$\text{Ni}_5\text{@Pt}$	323	110	4.5	75%	2.3	35
RhCl_3	323	180	4.1	68.3%	93.3	32
$\text{Ni}_{0.9}\text{Mo}_{0.1}$	323	1.5	3.0	50%	4998	17
$\text{Co NPs}/\text{PSSMA}$	313	40	3.0	50%	450	16
$\text{Ni}_{0.5}\text{Fe}_{0.5}\text{-CeO}_x/\text{MIL-101}$	343	4.27	6.0	100%	351	8
$\text{Ni}_{0.9}\text{Pt}_{0.1}/\text{MSC-30}$	303	4.5	6.0	100%	662	36

References:

- 1 D. C. Marcano, D. V. Kosynkin, J. M. Berlin, A. Sinitskii, Z. Sun, A. S. Slesarev, L. B. Alemany, W. Lu, J. M. Tour, *Acs Nano*,2018, **12** 2078-2078.
- 2 S.-J. Li, Y.-T. Zhou, X. Kang, D.-X. Liu, L. Gu, Q.-H. Zhang, J.-M. Yan, Q. Jiang, *Adv. Mater.*,2019, **31** 1806781.
- 3 X. Du, C. Liu, C. Du, P. Cai, G. Cheng, W. Luo, *Nano Research*,2017, **10** 2856-2865.
- 4 A. Kumar, X. Yang, Q. Xu, *J. Mater. Chem. A*, 2019, **7** 112-115.
- 5 L. Shang, B. Zeng, F. Zhao, *ACS Appl. Mater. Interfaces*,2015, **7** 122-128.
- 6 J.-M. Yan, S.-J. Li, S.-S. Yi, B.-R. Wulan, W.-T. Zheng, Q. Jiang, *Adv. Mater.*,2018, **30** 1703038.
- 7 G. Zhang, B. Y. Xia, X. Wang, X. W. Lou, *Adv. Mater.*,2014, **26** 2408-2412.
- 8 S.-J. Li, H.-L. Wang, B.-R. Wulan, X.-b. Zhang, J.-M. Yan, Q. Jiang, *Adv. Energy Mater.*,2018, **8** 1800625.
- 9 B. Dehghanzad, M. K. R. Aghjeh, O. Rafeie, A. Tavakoli, A. J. Oskooie, *Rsc Advances*,2016, **6** 3578-3585.
- 10 A. Chakravarty, K. Bhowmik, G. De, A. Mukherjee, *New J. Chem.*,2015, **39** 2451-2458.
- 11 S. K. Singh, Q. Xu, *Chem. Commun.*,2010, **46** 6545-6547.
- 12 B. Xiong, Y. Zhou, Y. Zhao, J. Wang, X. Chen, R. O'Hayre, Z. Shao, *Carbon*,2013, **52** 181-192.
- 13 D. W. Chang, H.-J. Choi, J.-B. Baek, *J. Mater. Chem. A*, 2015, **3** 7659-7665.
- 14 D. Deng, X. Pan, L. Yu, Y. Cui, Y. Jiang, J. Qi, W.-X. Li, Q. Fu, X. Ma, Q. Xue, G. Sun, X. Bao, *Chem. Mater.*,2011, **23** 1188-1193.
- 15 Q. Yao, Z.-H. Lu, Z. Zhang, X. Chen, Y. Lan, *Sci. Rep.*,2014, **4** 1-8.
- 16 S. Karahan, S. Ozkar, *Int. J. Hydrogen Energy*,2015, **40** 2255-2265.
- 17 K. Yang, Q. Yao, W. Huang, X. Chen, Z.-H. Lu, *Int. J. Hydrogen Energy*,2017, **42** 6840-6850.
- 18 J. Chen, Z.-H. Lu, Q. Yao, G. Feng, Y. Luo, *J. Mater. Chem. A*,2018, **6** 20746-20752.
- 19 M. Yurderi, T. Top, A. Bulut, G. S. Kanberoglu, M. Kaya, M. Zahmakiran, *Inorg. Chem.*,2020, **59** 9728-9738.
- 20 Q. Yao, M. He, X. Hong, X. Chen, G. Feng, Z.-H. Lu, *Int. J. Hydrogen Energy*,2019, **44** 28430-28440.
- 21 X. Hong, Q. Yao, M. Huang, H. Du, Z.-H. Lu, *Inorg. Chem. Front.*,2019, **6** 2271-2278.
- 22 Z. Zhang, S. Zhang, Q. Yao, G. Feng, M. Zhu, Z.-H. Lu, *Inorg. Chem. Front.*,2018, **5** 370-377.
- 23 Z. Zhang, S. Zhang, Q. Yao, X. Chen, Z.-H. Lu, *Inorg. Chem.*,2017, **56** 11938-11945.
- 24 H. Zou, S. Zhang, X. Hong, Q. Yao, Y. Luo, Z.-H. Lu, *J. Alloys Compd.*,2020, **835** 155426.
- 25 Z. Zhang, Z.-H. Lu, H. Tan, X. Chen, Q. Yao, *J. Mater. Chem. A*,2015, **3** 23520-23529.
- 26 S.-J. Li, X. Kang, B.-R. Wulan, X.-L. Qu, K. Zheng, X.-D. Han, J.-M. Yan, *Small Methods*,2018, **2** 1800250.
- 27 Z. Zhang, Z.-H. Lu, X. Chen, *ACS Sustainable Chem. Eng.*,2015, **3** 1255-1261.
- 28 Q. Yao, Z.-H. Lu, R. Zhang, S. Zhang, X. Chen, H.-L. Jiang, *J. Mater. Chem. A*,2018, **6** 4386-4393.
- 29 D.-C. Zhong, K. Aranishi, A. K. Singh, U. B. Demirci, Q. Xu, *Chem. Commun.*,2012, **48** 11945-11947.
- 30 K. Yang, K. Yang, S. Zhang, Y. Luo, Q. Yao, Z.-H. Lu, *J. Alloys Compd.*,2018, **732** 363-371.
- 31 Q. Yao, K. Yang, W. Nie, Y. Li, Z.-H. Lu, *Renew. Energy*,2020, **147** 2024-2031.
- 32 C. Cakanyildirim, U. B. Demirci, T. Sener, Q. Xu, P. Miele, *Int. J. Hydrogen Energy*,2012, **37** 9722-9729.
- 33 C. Li, Y. Dou, J. Liu, Y. Chen, S. He, M. Wei, D. G. Evans, X. Duan, *Chem. Commun.*,2013, **49** 9992-

9994.

- 34 Z. Zhang, Y. Wang, X. Chen, Z.-H. Lu, *J. Power Sources*, 2015, **291** 14-19.
- 35 D. Clemencon, J. F. Petit, U. B. Demirci, Q. Xu, P. Miele, *J. Power Sources*, 2014, **260** 77-81.
- 36 Q.-L. Zhu, D.-C. Zhong, U. B. Demirci, Q. Xu, *Acs Catalysis*, 2014, **4** 4261-4268.